

DMD2019-3309

TOWARDS FLEXIBLE STEERABLE INSTRUMENTS FOR OFFICE-BASED LARYNGEAL SURGERY

Kevin O'Brien

Department of Computer Science
Worcester Polytechnic Institute
Worcester, MA

Zachary R. Boyer

Robotics Engineering Program
Worcester Polytechnic Institute
Worcester, MA

Cory T. Brolliar

Robotics Engineering Program
Worcester Polytechnic Institute
Worcester, MA

Benjamin G. Mart

Robotics Engineering Program
Worcester Polytechnic Institute
Worcester, MA

Thomas L. Carroll

Harvard Medical School
Brigham and Women's Voice Program
Brigham and Women's Hospital
Boston, MA

Loris Fichera

Robotics Engineering Program and
Department of Computer Science
Worcester Polytechnic Institute
Worcester, MA

ABSTRACT

Office-based endoscopic procedures are becoming an increasingly attractive option for the treatment of laryngeal abnormalities, but their effectiveness is limited by the lack of articulation in currently available surgical instruments. In this paper, we propose the development of novel miniaturized steerable instruments aimed to overcome this limitation and extend a surgeon's reach inside the larynx. To guide the designs of these new instruments, we report on a simulation study which uses image-based anatomical models to derive the kinematic requirements to operate inside the laryngeal cavity.

INTRODUCTION

Laryngeal lesions, both benign and malignant, can cause speech impairment by interrupting the normal physiologic vibration of the vocal folds. Benign lesions alone (e.g. polyps, nodules or cysts) are prevalent in the general population with an estimated 3% of individuals affected [1]. Surgical removal of laryngeal lesions is normally performed in the operating room under general anesthesia [2], but new treatment protocols are currently being investigated to treat laryngeal disease in an office setting [3]. The main technological advancement that enabled the development of these new protocols is the progressive miniaturization of flexible chip-tip camera endoscopes, which are now commercially available in diameters suitable for trans-nasal use in conscious patients, as illustrated in Fig. 1(a). These endoscopes are equipped with a working channel which can be used

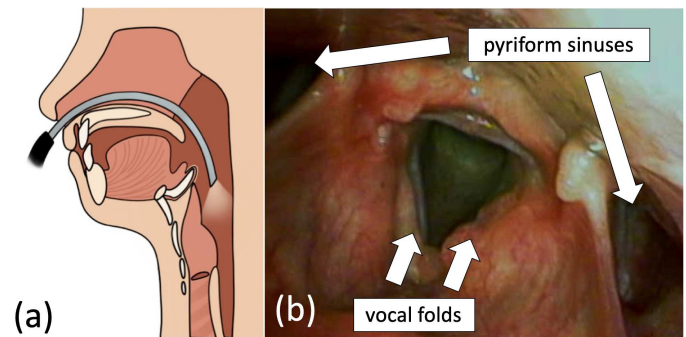


FIGURE 1. (A) TRANSNASAL ENDOSCOPY OF THE LARYNX; (B) INTRA-OPERATIVE VIEW, WITH PATHOLOGY APPEARING ON THE VOCAL FOLDS.

to deploy surgical instrumentation (e.g. a pair of miniaturized forceps or a laser fiber). The advantages of performing laryngeal surgery in the office are manifold: office procedures eliminate the need for general anesthesia (and its associated risks) [3], cost significantly less [4, 5] and involve a much shorter procedural time [5] when compared to procedures in the operating room.

Despite these benefits, in-office laryngeal surgery still presents several technical limitations which hinder routine application. One of the major challenges is represented by the restricted range of maneuvers attainable with available instrumentation [3, 6–8]; trans-nasal endoscopes can be made to bend in

different directions, but the small diameter of the working channel (typically ≤ 2 mm in diameter) does not permit the passage of instruments equipped with articulation mechanisms. Lack of instrument articulation creates two practical problems: (i) it makes it impossible to manipulate tissue without bending the endoscope, i.e. without constantly changing the field of vision — this makes manipulation unintuitive and often creates inadequate exposures of the surgical field [7]; (ii) it precludes access to those anatomical locations that cannot be reached in a linear path [6,7]. Relevant examples include the undersurface of the vocal folds and the *pyriform sinuses* (shown in Fig. 1(b)), a pair of cavities located lateral to and posterior to the voice box [9].

Aiming to overcome the issues outlined above, we propose exploring the creation of new surgical instrumentation for office-based laryngeal surgery. We envision the creation of miniaturized steerable tools that can be deployed through the operating channel of a trans-nasal endoscope. The tools will be equipped with distal bending in order to amplify a surgeon’s manipulation ability inside the larynx.

Creating steering instruments at the scale required for our application is not straightforward, as articulation mechanisms based on traditional linkages (e.g. ball/universal joints, cables and pulleys) can only be miniaturized to a certain extent [10]. Hoffman et al. recently investigated the use of a commercially-available steering sheath used in urology (diameter = 4.95 mm) to operate in the larynx [11]. This is a promising solution, but the diameter of the sheath is still not sufficiently small to allow insertion through the endoscope’s operating channel, and it creates

a requirement for a second operator to hold and manipulate the sheath. We propose tackling these challenges by exploring the use of miniaturized tube-like continuum bending mechanisms. Curved bending sections can be realized in the body of a thin tube via the creation of notches and the attachment of a pull-wire at the tip [12]. Different tube materials have been demonstrated in the literature, including super-elastic Nickel-Titanium (NiTi) [12, 13] and polyether ether ketone (PEEK) [14]. These bending mechanisms present two characteristics that make them particularly attractive for our application: they can be manufactured in tiny diameters (< 2 mm was demonstrated in [12–15]), and they have a hollow lumen (i.e. the inner diameter of the tube) which can be used to pass instruments.

As a first step in our investigation, we present a study aiming to establish general kinematic requirements for instrument operation in the larynx. Using three-dimensional anatomical models of the laryngeal cavity, we simulate the insertion and manipulation of steerable instruments with varying degrees of freedom. We define volume and visibility-based metrics to evaluate how well a given design can cover the laryngeal anatomy.

METHODS

Our simulation framework is illustrated in Fig. 2. Three-dimensional anatomical models of the larynx are generated based on Computed Tomography (CT) scans of real patients. These models are used as a virtual environment where we simulate the deployment of steerable instruments. In the following sections,

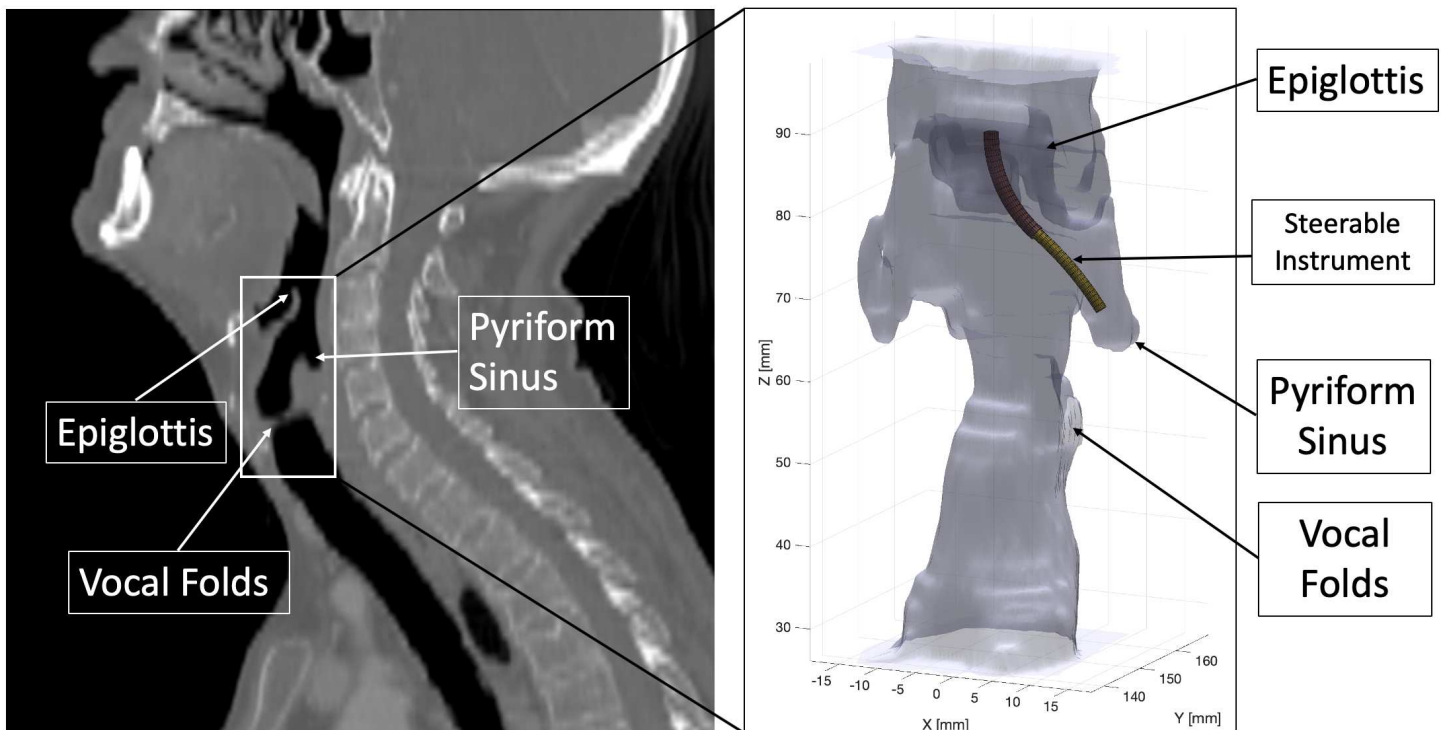


FIGURE 2. (LEFT) SEGMENTATION OF THE LARYNX ANATOMY IN COMPUTED TOMOGRAPHY SCANS; (RIGHT) VIRTUAL STEERABLE INSTRUMENT DEPLOYED IN A THREE-DIMENSIONAL MODEL OF THE LARYNX.

we first outline the protocol used to generate the larynx anatomical models and the kinematic model employed to simulate instrument motion. We then describe experimental work aimed to quantify the number of individual degrees of freedom required to maximize an instrument’s reach within the larynx.

Three-Dimensional Larynx Models

The CT scans used in this study were selected from the Cancer Genome Atlas Head-Neck Squamous Cell Carcinoma (TCGA-HNSC) dataset [16], a large multi-institution collection of data regarding patients diagnosed with malignant tumors of the head and neck. The procedure used to generate a 3D larynx model from a CT scan is as follows: we first visually identify the larynx anatomy in the sagittal plane using 3D Slicer [17] (see Fig. 2), then we crop the CT volume to include the tract of the upper airway going from the epiglottis down to the sub-glottic region (i.e. below the vocal folds), finally, we use the segmentation function of 3D Slicer to generate a three-dimensional rendering of the cropped volume, which is exported as a stereolithography (STL) model.

Instrument Kinematic Model

The kinematics of continuum bending mechanisms have been extensively investigated in prior work [18]. Assuming no external loading, the shape of these devices can be modeled as a sequence of individual curved links, each characterized by a length ℓ_j , a curvature k_j and an axial rotation ϕ_j (as shown in Fig. 3.). For a single link, the homogeneous transformation matrix T between the base and the tip can be calculated using the following product of exponentials:

$$T(k_j, \phi_j, \ell_j) = e^{\hat{S}_1 \phi_j} e^{\hat{S}_2 k_j \ell_j} \quad (1)$$

where $S_1 = [0 \ 0 \ 0 \ 0 \ 0 \ 1]^T$ and $S_2 = [0 \ 0 \ 1/k_j \ 0 \ 1 \ 0]^T$. The operator $\hat{\cdot}$ that appears in Eqn.(1) maps twists from \mathbb{R}^6 to elements of $\mathfrak{se}(3)$, i.e. the Lie Algebra of the special Euclidean group SE(3). Without loss of generality, in this paper we assume that arc parameters k_j , ϕ_j and ℓ_j can be directly controlled. Our framework can be easily extended to account for any mechanism-specific mapping between actuator variables and arc parameters.

ANALYSIS OF KINEMATIC REQUIREMENTS

Continuum bending mechanisms can be designed to incorporate an arbitrary sequence of curved links, each having independent degrees of freedom. Intuitively, adding more links will increase the overall dexterity of the mechanism, but it will make it more complex to manufacture and control. One question that naturally arises is then *how many individual links are necessary for our application?* A single curved link may be sufficient to reach any arbitrary point in the larynx (assuming the point falls within actuation limits and that no obstacles are in the way). However, we suspect that adding a second distal link (as shown in Fig. 4) might enable more extensive access to tissue.

To verify the validity of this hypothesis, we simulated the deployment of two different instruments — one made of a single steerable link, the second composed of two independent links – and compared the volume and extent of tissue surface reachable by each of them. Instrument motion was simulated through a sampling-based motion planning algorithm (rapidly-expanding random trees - RRT [19]). To account for anatomical variability among different patients, we performed simulations on a total of five different larynx models extracted from the TCGA-HNSC dataset. Three males and two females were involved in the study.

Reachable Volume Estimation To estimate the extent of volume that can be reached by a given instrument, we use an approach similar to that described in [20]. We first execute RRT to generate a large number (10,000) of locations that can be reached in a collision-free path (see Fig. 5). RRT provides probabilistic completeness, meaning that the longer the algorithm is run, the more likely it is that it will cover the true reachable volume entirely. In our simulations, RRT operates on the arc parameters k_j , ϕ_j and ℓ_j of each individual link, which are left to vary freely within the boundaries specified in Table 1. The MATLAB `boundary` function is used to calculate the tightest single-region boundary around the points generated by RRT, and to estimate its corresponding volume.

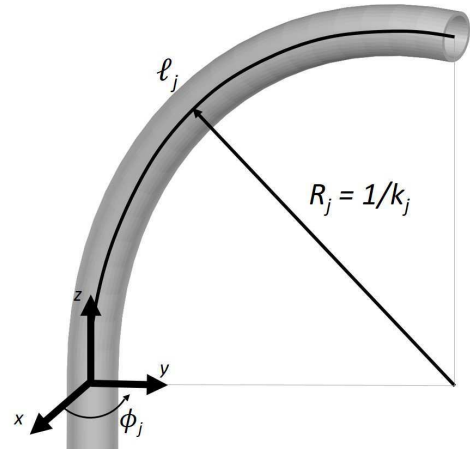


FIGURE 3. KINEMATICS OF SINGLE CONTINUUM LINK.

TABLE 1. RANGE OF ARC PARAMETERS USED IN SIMULATION

	k_j (mm^{-1})		ϕ_j (rad)		ℓ (mm)	
	min	max	min	max	min	max
One link	0	0.1	0	2π	0	50
Two links	0	0.1	0	2π	0	25

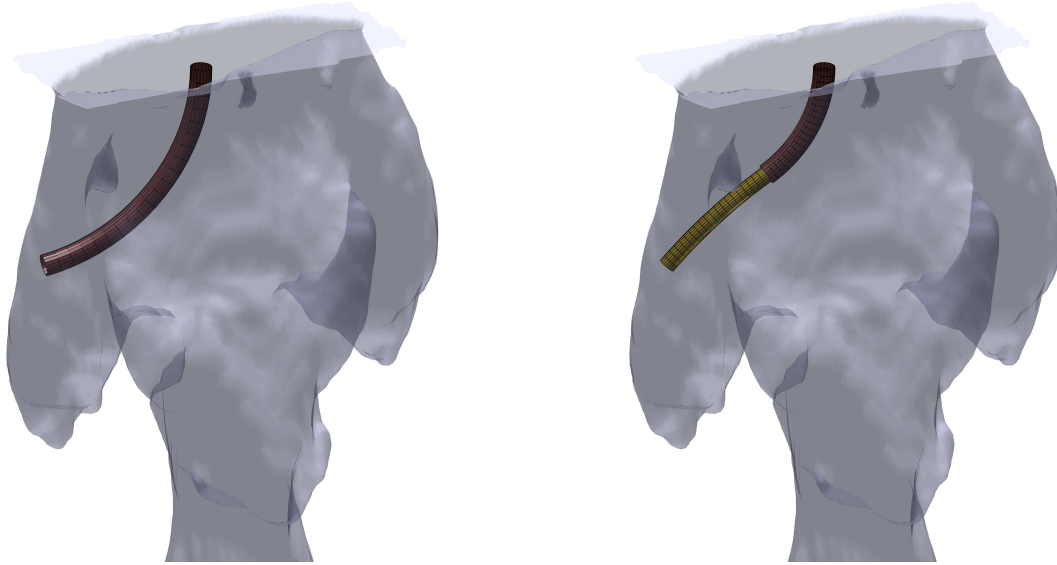


FIGURE 4. 1-LINK (LEFT) AND 2-LINK (RIGHT) INSTRUMENTS.

Visible Surface Estimation Estimation of visible tissue surface is performed as follows. We first consider the set of reachable points generated by RRT and select only those points that are in close proximity to tissue — arbitrarily defined as being within a 5 mm distance from the internal surface of the larynx. For each of these points, we generate visibility maps using the Hidden Point Removal operator [21], combined with a ray-casting procedure that narrows down visibility within a 20° cone projecting from the tip of the instrument. Sample visibility maps calculated with this approach are shown in Fig. 6.

RESULTS

Table 2 summarizes the results of the volume estimation procedure. The two-link design was found to provide slightly higher volume coverages in four of the five models. The average difference in volume coverage (absolute value) was found to be 0.76 cm^3 .

Estimations of reachable surface are reported in Table 3. In all five patients, the two-link design was found to be able to visualize a larger amount of surface area. The average difference in visible surface across the five patients was 4.76 cm^2 .

DISCUSSION

Experimental results seem to support the hypothesis that a design with two curved links does not provide a significant improvement in terms of reachable volume when compared to a single link instrument. However, a measurable improvement was detected in the analysis of the reachable surface area. Visual analysis of the visibility maps reveals that the improvement is particularly marked in challenging locations like the pyriform sinuses. The two-link design was able to visualize a higher portion of the sinuses, including the bottom of these cavities (see

TABLE 2. RESULTS OF THE VOLUME COVERAGE EXPERIMENTS

Patient ID	One Link (cm^3)	Two Links (cm^3)
1	6.06	5.88
2	6.72	6.96
3	4.32	4.99
4	5.97	7.93
5	8.27	9.04

TABLE 3. RESULTS OF THE SURFACE AREA COVERAGE EXPERIMENTS

Patient ID	One Link (cm^2)	Two Links (cm^2)
1	14.21	20.61
2	19.68	22.55
3	14.10	19.30
4	19.95	25.86
5	19.93	23.34

Fig. 6), something that can be attributed to the fact that a two-link instrument can approach a prescribed location with arbitrary orientation.

One obvious limitation of this study is that it involved exper-

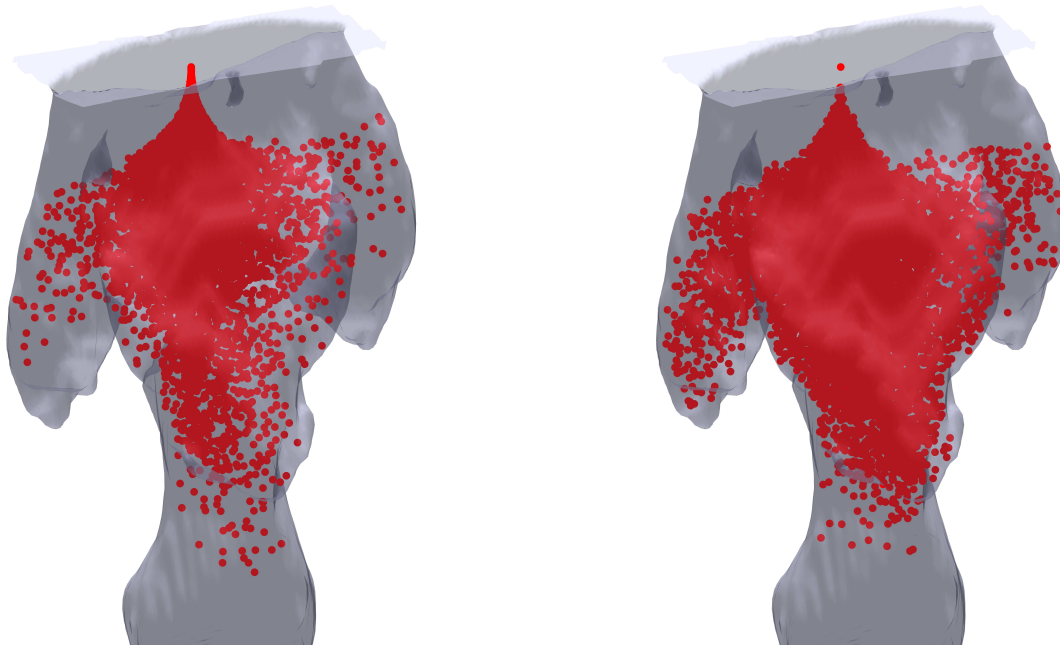


FIGURE 5. REACHABLE POINTS WITH 1-LINK (LEFT) AND 2-LINK (RIGHT) INSTRUMENTS.

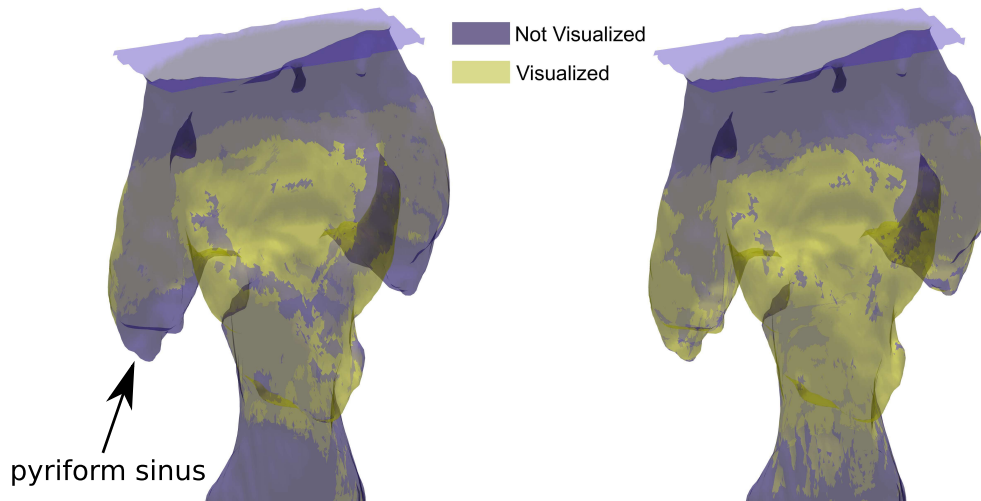


FIGURE 6. VISIBLE SURFACE WITH 1-LINK (LEFT) AND 2-LINK (RIGHT) INSTRUMENTS.

imentation on a limited number of larynx models, and therefore it may not have sufficiently accounted for inter-patient anatomical variability. Additional analysis and simulations involving a larger number of patient models will be conducted in the future to verify whether our findings can be applied to the general patient population.

In future work, we plan to utilize the framework described in this study to inform the design and fabrication of prototype instruments for endoscopic laryngeal surgery. The next immediate step will involve building the prototype of an actual tool — e.g. a steerable laser fiber — and validating it in-vitro. Additional research will have to be conducted to design a control interface to enable intuitive surgeon operation of the proposed instruments.

ACKNOWLEDGMENTS

The results shown here are in whole or part based upon data generated by the TCGA Research Network: <http://cancergenome.nih.gov/>.

REFERENCES

- [1] Hah, J. H., Sim, S., An, S.-Y., Sung, M.-W., and Choi, H. G., 2015. “Evaluation of the prevalence of and factors associated with laryngeal diseases among the general population”. *The Laryngoscope*, **125**(11), pp. 2536–2542.
- [2] Steiner, W., Ambrosch, P., and Braun, U., 2000. *Endoscopic laser surgery of the upper aerodigestive tract*:

- with special emphasis on cancer surgery, Vol. 1. Thieme Stuttgart.
- [3] Wellenstein, D. J., Schutte, H. W., Takes, R. P., Honings, J., Marres, H. A., Burns, J. A., and van den Broek, G. B., 2018. "Office-based procedures for the diagnosis and treatment of laryngeal pathology". *Journal of Voice*, **32**(4), pp. 502–513.
 - [4] Rees, C. J., Postma, G. N., and Koufman, J. A., 2007. "Cost savings of unsedated office-based laser surgery for laryngeal papillomas". *Annals of Otolaryngology, Rhinology & Laryngology*, **116**(1), pp. 45–48.
 - [5] Hillel, A. T., Ochsner, M. C., Johns III, M. M., and Klein, A. M., 2016. "A cost and time analysis of laryngology procedures in the endoscopy suite versus the operating room". *The Laryngoscope*, **126**(6), pp. 1385–1389.
 - [6] Del Signore, A. G., Shah, R. N., Gupta, N., Altman, K. W., and Woo, P., 2016. "Complications and failures of office-based endoscopic angiolytic laser surgery treatment". *Journal of Voice*, **30**(6), pp. 744–750.
 - [7] Hu, H.-C., Lin, S.-Y., Hung, Y.-T., and Chang, S.-Y., 2017. "Feasibility and associated limitations of office-based laryngeal surgery using carbon dioxide lasers". *JAMA Otolaryngology–Head & Neck Surgery*, **143**(5), pp. 485–491.
 - [8] Hwang, S. M., Lee, D. Y., Im, N.-R., Lee, H.-J., Kim, B., Jung, K.-Y., Kim, T. H., and Baek, S.-K., 2015. "Office-based laser surgery for benign laryngeal lesion". *Medical Lasers; Engineering, Basic Research, and Clinical Application*, **4**(2), pp. 65–69.
 - [9] Hamoir, M., Fievez, J., Schmitz, S., Velasco, D., and Lengele, B., 2013. "Extended voice-sparing surgery in selected pyriform sinus carcinoma: Techniques and outcomes". *Head & neck*, **35**(10), pp. 1482–1489.
 - [10] Jelínek, F., Arkenbout, E. A., Henselmans, P. W., Pessers, R., and Breedveld, P., 2015. "Classification of joints used in steerable instruments for minimally invasive surgery—a review of the state of the art". *Journal of Medical Devices*, **9**(1), p. 010801.
 - [11] Hoffman, H. T., Stegall, H., Wingler, T., and Blitzer, A., 2018. "Steering sheath for 2-nostril transnasal office laryngoscopy". *Annals of Otolaryngology, Rhinology & Laryngology*, **127**(2), pp. 99–104.
 - [12] Swaney, P. J., York, P. A., Gilbert, H. B., Burgner-Kahrs, J., and Webster, R. J., 2017. "Design, fabrication, and testing of a needle-sized wrist for surgical instruments". *Journal of medical devices*, **11**(1), p. 014501.
 - [13] Francis, P., Eastwood, K., Bodani, V., Looi, T., and Drake, J., 2018. "Design, modelling and teleoperation of a 2 mm diameter compliant instrument for the da vinci platform". *Annals of biomedical engineering*, pp. 1–13.
 - [14] Rox, M., Riojas, K., Emerson, M., Oliver-Butler, K., Rucker, D. C., and Webster, R. J., 2018. "Luminal robots small enough to fit through endoscope ports: initial tumor resection experiments in the airways". In *Proceedings of the Hamlyn Symposium on Medical Robotics 2018*, pp. 63–64.
 - [15] Fichera, L., Dillon, N. P., Zhang, D., Godage, I. S., Siebold, M. A., Hartley, B. I., Noble, J. H., Russell, P. T., Labadie, R. F., and Webster, R. J., 2017. "Through the eustachian tube and beyond: A new miniature robotic endoscope to see into the middle ear.". *IEEE robotics and automation letters*, **2**(3), pp. 1488–1494.
 - [16] Zuley, M., Jarosz, R., Kirk, S., Lee, Y., Colen, R., Garcia, K., and Aredes, N., 2017. Radiology data from the cancer genome atlas head-neck squamous cell carcinoma [tcga-hnsc] collection.
 - [17] Fedorov, A., Beichel, R., Kalpathy-Cramer, J., Finet, J., Fillion-Robin, J.-C., Pujol, S., Bauer, C., Jennings, D., Fennessy, F., Sonka, M., et al., 2012. "3d slicer as an image computing platform for the quantitative imaging network". *Magnetic resonance imaging*, **30**(9), pp. 1323–1341.
 - [18] Webster, R. J., and Jones, B. A., 2010. "Design and kinematic modeling of constant curvature continuum robots: A review". *The International Journal of Robotics Research*, **29**(13), pp. 1661–1683.
 - [19] LaValle, S. M., 2006. *Planning algorithms*. Cambridge university press.
 - [20] Baykal, C., Torres, L. G., and Alterovitz, R., 2015. "Optimizing design parameters for sets of concentric tube robots using sampling-based motion planning". In *Intelligent Robots and Systems (IROS), 2015 IEEE/RSJ International Conference on*, IEEE, pp. 4381–4387.
 - [21] Katz, S., Tal, A., and Basri, R., 2007. "Direct visibility of point sets". In *ACM Transactions on Graphics (TOG)*, Vol. 26, ACM, p. 24.